# Two-dimensional infrared spectroscopy and ultrafast anisotropy decay of water

Jansen, T. L. C.; Auer, B. M.; Yang, Mino; Skinner, J. L.

*Published in:*
Journal of Chemical Physics

*DOI:*
10.1063/1.3454733

# Two-dimensional infrared spectroscopy and ultrafast anisotropy decay of water

T. l. C. Jansen, B. M. Auer, Mino Yang, and J. L. Skinner

Citation: The Journal of Chemical Physics **132**, 224503 (2010); doi: 10.1063/1.3454733
View online: https://doi.org/10.1063/1.3454733
View Table of Contents: http://aip.scitation.org/toc/jcp/132/22
Published by the American Institute of Physics

# Two-dimensional infrared spectroscopy and ultrafast anisotropy decay of water

T. l. C. Jansen,[1,a)] B. M. Auer,[2] Mino Yang,[2,3] and J. L. Skinner[2]
[1]*Center for Theoretical Physics and Zernike Institute for Advanced Materials, University of Groningen, Nijenborgh 4, 9747 AG Groningen, The Netherlands*
[2]*Department of Chemistry and Theoretical Chemistry Institute, University of Wisconsin, Madison, Wisconsin 53706, USA*
[3]*Department of Chemistry and Basic Sciences Research Institute, Chungbuk National University, Cheongju, Chungbuk 361-763, Republic of Korea*

(Received 17 February 2010; accepted 26 May 2010; published online 9 June 2010)

We introduce a sparse-matrix algorithm that allows for the simulation of two-dimensional infrared (2DIR) spectra in systems with many coupled chromophores. We apply the method to bulk water, and our results are based on the recently developed *ab initio* maps for the vibrational Hamiltonian. Qualitative agreement between theory and experiment is found for the 2DIR spectra without the use of any fitting or scaling parameters in the Hamiltonian. The calculated spectra for bulk water are not so different from those for HOD in $D_2O$, which we can understand by considering the spectral diffusion time-correlation functions in both cases. We also calculate the ultrafast anisotropy decay, which is dominated by population transfer, finding very good agreement with experiment. Finally, we determine the vibrational excitation diffusion rate, which is more than two orders of magnitude faster than the diffusion of the water molecules themselves. © *2010 American Institute of Physics*. [doi:10.1063/1.3454733]

## I. INTRODUCTION

Two-dimensional infrared (2DIR) spectroscopy has proven to be an efficient tool for investigating ultrafast dynamics in complex systems. Experimentally, the method has been applied to small systems with only one or a few coupled vibrations,[1–3] to large proteins with numerous coupled vibrations,[2,4–6] and to bulk water,[7] where at least formally an infinite number of vibrations are coupled. When there is only a single chromophore, spectral simulation is straightforward.[3] Theoretical simulations have also been able to address systems with several coupled chromophores in a quite satisfactory way with the numerical integration of the Schrödinger equation (NISE) approach.[8–10] This method was successfully applied to a small $\beta$-hairpin.[11] For larger systems, a time-averaging approximation (TAA) has been suggested.[12,13] While it is faster than the NISE method, it still requires diagonalization of the double-excited states, which is the bottleneck of the NISE scheme.[8,9]

Paarmann *et al.*[14,15] devised an efficient propagation scheme for the double-excited states within the NISE approach. This allowed for application to a system of 128 coupled OH stretch vibrations of water. In the meantime, an efficient method based on the propagation of the nonlinear exciton equations was developed, further decreasing the required simulation time.[16] Another alternative for obtaining the nonlinear response function is based on nonequilibrium molecular dynamics (MD).[17,18] This method treats the problem completely classically and therefore only applies when the thermal energy is high compared to the relevant transition energies. Since in water the OH stretch energy is significantly higher than the thermal energy at room temperature, a quantum treatment of those degrees of freedom is needed. It should be noted that the NISE method is also a high-temperature approximation, which only applies when the spectral bandwidth is small compared to the thermal energy.[8] In the present paper, we introduce the use of a sparse-matrix approximation that allows for a further speedup of the original NISE algorithm and makes it applicable to even larger systems. We apply the method to bulk water.

To simulate the spectra of HOD in $H_2O$ and bulk water, mappings connecting the local structure as found in MD simulations with the vibrational Hamiltonian were developed. The first HOD maps directly combined intramolecular force fields with the MD force field.[19,20] Later approaches assumed that the origin of the frequency shift induced by the solvent is electrostatic and employed a Stark shift approximation.[21] It was found that parametrizations based on *ab initio* calculations on water clusters[22] or water molecules exposed to electric fields[23] reproduced the HOD in $H_2O$ spectra quite well. These maps were then extended to bulk water using the same mapping principles as for HOD.[15,24] In the present paper, a mapping for $H_2O$ that has already been demonstrated to catch the IR and Raman spectral features of bulk water very well will be used.[24]

2DIR spectra and ultrafast anisotropy decay of bulk water have previously been studied both experimentally[7,25,26] and theoretically.[14,15,27] The 2DIR experiments have been difficult to interpret since several competing processes (spectral diffusion, energy transfer, and vibrational relaxation) all occur on similar time scales. In terms of theory, Paarmann *et al.*[14,15] calculated the 2DIR spectrum, while Torii[27] investi-

[a)]Electronic mail: thomas.lacour@gmail.com.

 

gated the population transfer between the OH stretch vibrations. In the 2DIR simulations,[14,15] an electrostatic map for the molecular eigenstates was used, which results in an adiabatic treatment of the intramolecular population transfer. Transition dipole interactions led to the intermolecular coupling. The calculated frequency and coupling maps were both scaled to match experimental observables. Torii[27] also used an electrostatic frequency map, but in the site representation, and neglected the intramolecular coupling. The latter prevents direct transfer of population between the two OH vibrations within the same molecule. The intermolecular coupling was determined by transition dipole interactions.

In this paper, we present theoretical 2DIR spectra and anisotropy decay calculations for bulk water by combining MD simulations with *ab initio* maps to produce the vibrational Hamiltonian[24,28] and NISE to obtain the spectra.[9] In our Hamiltonian, maps for the site frequencies and the intramolecular coupling are used, which provide a full nonadiabatic treatment of the intramolecular population dynamics. Furthermore, the diagonal anharmonicity and the 1-2 transition dipole are also described with *ab initio* maps,[28] and the coupling between OH stretches in different water molecules is found by optimizing the position of the transition dipole to results from *ab initio* calculations on water clusters.[24] This leaves us with a complete map for the vibrational Hamiltonian without any free parameters. With this Hamiltonian excellent results were obtained for the linear absorption and Raman spectra in bulk water,[24,28,29] the sum-frequency generation spectra at the water liquid/vapor interface,[30,31] and the 2DIR spectra of water dissolved in acetonitrile.[32]

We find good agreement between theory and experiment for bulk water, for both 2DIR spectra and anisotropy decay. To understand the relevant time scales in these experiments, it is useful to contrast $H_2O$, with dilute HOD in $D_2O$, where analogous experiments have also been performed.[3] In the latter case, frequency mismatches ensure that the OH stretch chromophore is isolated. Therefore, a primary difference between these two systems is vibrational coupling (in $H_2O$), which produces vibrational energy transfer and which, in principle, leads to enhanced spectral diffusion and anisotropy decay. Comparison between these two sets of experiments shows that anisotropy decay is dramatically faster in $H_2O$, while spectral diffusion, as manifested in the 2DIR lineshape, is only modestly faster. We explain this puzzle by considering the frequency time-correlation function (TCF), with and without vibrational coupling, and arguing that energy transfer produces greater anisotropy decay than spectral diffusion since vibrational coupling leads to effective energy transfer only to near-resonant chromophores.

## II. METHODS

MD simulations of $H_2O$ were performed on 128 SPC/E (Ref. 33) molecules in the NVE ensemble at 298 K. Snapshots were saved every 10 fs along a 200 ps trajectory. We describe the OH stretch vibrations quantum mechanically with a fluctuating vibrational Hamiltonian of the form

$$H(t) = \sum_i \omega_i(t) B_i^\dagger B_i + \sum_{i,j} J_{ij}(t) B_i^\dagger B_j - \sum_i \frac{\Delta_i(t)}{2} B_i^\dagger B_i^\dagger B_i B_i + \sum_i \vec{\mu}_i(t) \cdot \vec{E}(t)(B_i^\dagger + B_i) + \sum_i \vec{\mu}_i^{12}(t) \cdot \vec{E}(t)(B_i^\dagger B_i^\dagger B_i + B_i^\dagger B_i B_i). \quad (1)$$

Here, $B_i^\dagger$ and $B_i$ are bosonic creation and annihilation operators. The fundamental frequency $\omega_i$ for each OH stretch is determined from an electronic structure-based electrostatic map relating it to the electric field generated by the surrounding water molecules along the OH bond.[28] When $i$ and $j$ denote OH stretches within the same molecule, $J_{ij}$ is the intramolecular coupling, which is determined by an electrostatic map depending on the electric fields along both OH bonds.[24] If $i$ and $j$ are OH stretches on different water molecules, $J_{ij}$ is the intermolecular coupling determined by the transition dipole interaction.[24] The anharmonicity $\Delta_i$ and the transition dipoles $\vec{\mu}$ and $\vec{\mu}^{12}$ are determined by an electrostatic map depending on the electric field along the OH bond.[28] $\vec{\mu}^{12}$ is related to the difference between the ground-state to single-excited-state and the single-excited-state to double-excited-state transition dipoles. The former is $\vec{\mu}$ and the latter is $\sqrt{2}(\vec{\mu}+\vec{\mu}^{12})$.

The spectra were obtained with a version of the NISE method[9] adapted to large systems. The state of the quantum system is determined by the wave function $\Phi$ for the OH vibrations. The evolution of the quantum system is described by the time-dependent Schrödinger equation,

$$\frac{\partial}{\partial t}\Phi(t) = -\frac{i}{\hbar} H(t)\Phi(t). \quad (2)$$

This cannot be solved analytically when the Hamiltonian is not constant in time. However, a numerical approximation can be obtained by dividing the time into sufficiently short time intervals during which the Hamiltonian can safely be assumed to be constant. In that case, the solution for each interval is given by the solution of the time-dependent Schrödinger equation with time-independent Hamiltonian,

$$\Phi(t+\Delta t) \equiv U(t+\Delta t, t)\Phi(t) = \exp\left(-\frac{i}{\hbar} H(t)\Delta t\right)\Phi(t). \quad (3)$$

The time-evolution operator $U(t+\Delta t, t)$ then describes the time evolution during one such time interval. The time evolution for a longer time period is then simply given by the time-ordered product of the time-evolution operators for the intermediate time intervals. The time-evolution operators are combined with the transition dipoles to evaluate the response functions derived from time-dependent perturbation theory that govern the 2DIR spectra. In short, the state of the system is propagated with the time-evolution operators and when the system interacts with the laser field the excitation level of the propagated wave function is instantaneously raised or lowered by one. The expressions for the response functions are given in Eq. (11) of Ref. 9 and the scheme is discussed in more detail elsewhere.[8]

A split-operator approximation and a sparse-matrix scheme were employed to allow the application of the method to this system with a large number of oscillators. When no external electric field is present, states with different numbers of excitations are decoupled in the Hamiltonian in Eq. (1). The time-evolution operators for the single-excited and double-excited states can therefore be found independently. For the single-excited states, the time-evolution operator is then found by diagonalizing the Hamiltonian in the basis of the single-excited states. The matrix exponential is trivial in the eigenbasis and the time-evolution operator for the single-excited states is obtained when transforming back to the site basis.

The split-operator approximation is used to calculate the time-evolution operator for the double-excited states using

$$U^{(2)}_{ab;cd}(t+\Delta t,t) = \langle ac|U^{(2)}|bd\rangle, \quad |ac\rangle = \frac{1}{\sqrt{1+\delta_{ac}}} B^\dagger_a B^\dagger_c |0\rangle. \tag{4}$$

If the time-evolution operator for the single-excited states with a time interval $\Delta t$ is given by $U^{(1)}_{ab}(t+\Delta t,t)$, in the site basis the harmonic part of the double-excited time-evolution operator is[15]

$$\begin{aligned} U^{(2,H)}_{ab;cd}(t+\Delta t,t) = {} & \frac{1}{\sqrt{1+\delta_{ac}}\sqrt{1+\delta_{bd}}} (U^{(1)}_{ab}(t+\Delta t,t) \\ & \times U^{(1)}_{cd}(t+\Delta t,t) + U^{(1)}_{ad}(t+\Delta t,t) \\ & \times U^{(1)}_{cb}(t+\Delta t,t)). \end{aligned} \tag{5}$$

Paarmann *et al.*[14,15] approximated the anharmonic part of the time-evolution operator with

$$U^{(2,A)}_{ab;cd}(t+\Delta t,t) = \left(\delta_{ab}\delta_{cd} - \frac{i}{\hbar} H^A_{ab;cd}(t)\Delta t\right), \tag{6}$$

where $H^A(t)$ is the rather sparse anharmonic part of the Hamiltonian. In our case the anharmonic part of the Hamiltonian is diagonal because we do not include anharmonicites in the transition dipole coupling that arise the overtone transition dipoles do not exactly fulfill the harmonic rule (i.e., that the overtone dipole is given by $\sqrt{2}$ times the transition dipole of the fundamental transition), as was done in Refs. 14 and 15. We therefore used the matrix exponential, which is trivial to calculate in this case. The total time-evolution operator for the double-excited states is then given by the split-operator approximation,

$$\begin{aligned} U^{(2)}_{ab;cd}(t+\Delta t,t) = {} & U^{(2,A)}_{ab;cd}(t+\Delta t/2,t) U^{(2,H)}_{ab;cd}(t+\Delta t,t) \\ & \times U^{(2,A)}_{ab;cd}(t+\Delta t/2,t). \end{aligned} \tag{7}$$

In practice, these matrices are never multiplied with each other but rather are multiplied successively on a vector, which is computationally much more efficient.

The evaluation of the double-excited-state propagation is still very time consuming even when the split-operator approach is employed. We therefore made use of the fact that for large systems the time-evolution operator contains many small elements. We discarded elements of the single-excited-state propagator for which the absolute value squared was below a threshold $\epsilon$,

$$|U^{(1)}_{ab}(t+\Delta t,t)|^2 < \epsilon. \tag{8}$$

The value of $\epsilon$ must be selected sufficiently small that nothing important is thrown away, but large enough that most irrelevant elements of the time-evolution operator are not included in the simulation. Only during the waiting time the exact time-evolution operator was used. $\epsilon$ was set to $1.4 \times 10^{-10}$, which means that about 50% of the time-evolution matrix elements are neglected. Since the bottleneck in the calculation is the application of the harmonic part of the double-excited time-evolution operator and this depends on products of pairs of single-excited time-evolution operators, the speedup in this case is about a factor of 4. In less strongly coupled systems, significantly higher speedups can be expected.

The NISE method can be used to calculate not only the linear absorption and 2DIR spectra but also the population-transfer rate, the vibrational excitation diffusion, vibrational spectral diffusion, and the anisotropy decay. These quantities are useful for interpreting the spectra and analyzing the system properties. To investigate population transfer, we consider the population still remaining in an initially excited state, which is

$$P(t) = \langle |U^{(1)}_{jj}(t,0)|^2 \rangle. \tag{9}$$

The brackets indicate an ensemble average (a time average over the trajectory and an average over all chromophores). We will denote this as the population decay. Population transfer also results in a spread of the excitation wave packet, and it is interesting to know how the probability of detecting the excitation at different distances from the original excitation depends on time. The mean-square displacement of the probability wave is

$$\mathrm{MSD}(t) = \left\langle \sum_i |\vec{r}_i(t) - \vec{r}_j(0)|^2 |U^{(1)}_{ij}(t,0)|^2 \right\rangle. \tag{10}$$

Here, $\vec{r}_i$ is the position (taken to be the position of the hydrogen atom) of site $i$ at a given time. The diffusion of the probability density wave can be determined using the Einstein relation $\mathrm{MSD}(t)=6Dt$ for $t\to\infty$. If there is no population transfer, the MSD will reflect the diffusion of water molecules.

Spectral diffusion can be understood in terms of frequency TCFs. If there is no vibrational coupling, then one is simply interested in

$$C(t) = \langle \delta\omega_j(t)\, \delta\omega_j(0) \rangle, \tag{11}$$

where $\delta\omega_j(t)$ is the deviation of the frequency of the $j$th chromophore from its average value. When the vibrations are coupled, the frequency TCF becomes

$$C_P(t) = \left\langle \sum_i \delta\omega_i(t)\, \delta\omega_j(0) |U^{(1)}_{ij}(t,0)|^2 \right\rangle. \tag{12}$$

When there is no population transfer, this reduces to the normal (site) frequency TCF [Eq. (11)].

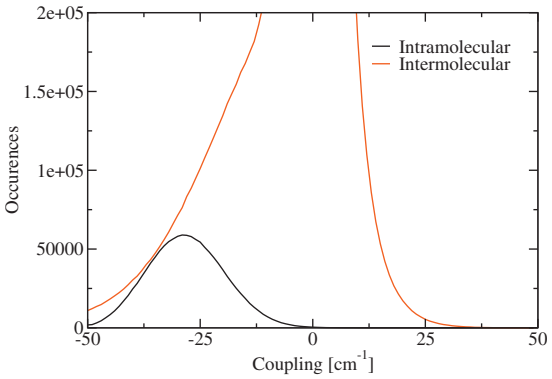


FIG. 1. The histogram shows the distribution of the intra- and intermolecular couplings.

The anisotropy decay can be obtained from the simulated/experimental signal in the parallel ($S_{\parallel}$) and perpendicular ($S_{\perp}$) polarization configurations, from

$$R(t) = \frac{S_{\parallel}(t) - S_{\perp}(t)}{S_{\parallel}(t) + 2S_{\perp}(t)}, \tag{13}$$

where $t$ is the time between pump and probe pulses. The experiments of interest[25,26] use very short pump pulses so that OH stretch modes of any frequency are excited, and the probe signal is integrated over all frequencies, which means that we do not have to worry about the frequency dependence, as indicated above. Thus, we calculate the anisotropy decay using the third-order response functions, but setting $t_1$ and $t_3$ to zero.[9]

## III. RESULTS

The distribution of intra- and intermolecular couplings is shown in Fig. 1. The average intramolecular coupling is $-27$ cm$^{-1}$. For most pairs of OH stretches, the intermolecular coupling is close to zero, but values close to that of typical intramolecular couplings occur about once for each OH stretch. In Fig. 2 we present the linear absorption spectrum calculated with the NISE and TAA methods, along with the experimental bulk water spectrum.[34] The NISE and TAA spectra are very similar and demonstrate the accuracy of the TAA method for calculating the linear absorption.[12,29] The interpretation of the linear spectrum is discussed in more detail in recent papers.[24,29]

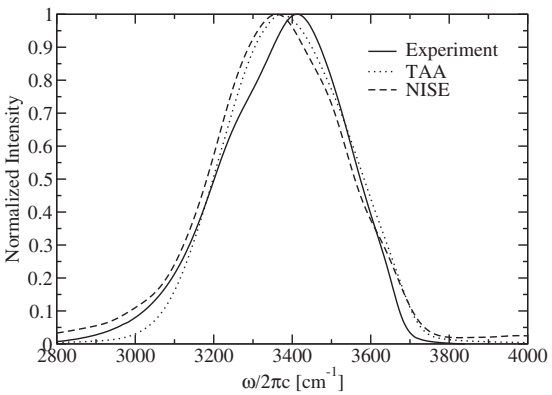


FIG. 2. The linear absorption spectra calculated with the TAA (taken from Ref. 12) and NISE methods compared with the experimental data (Ref. 34).

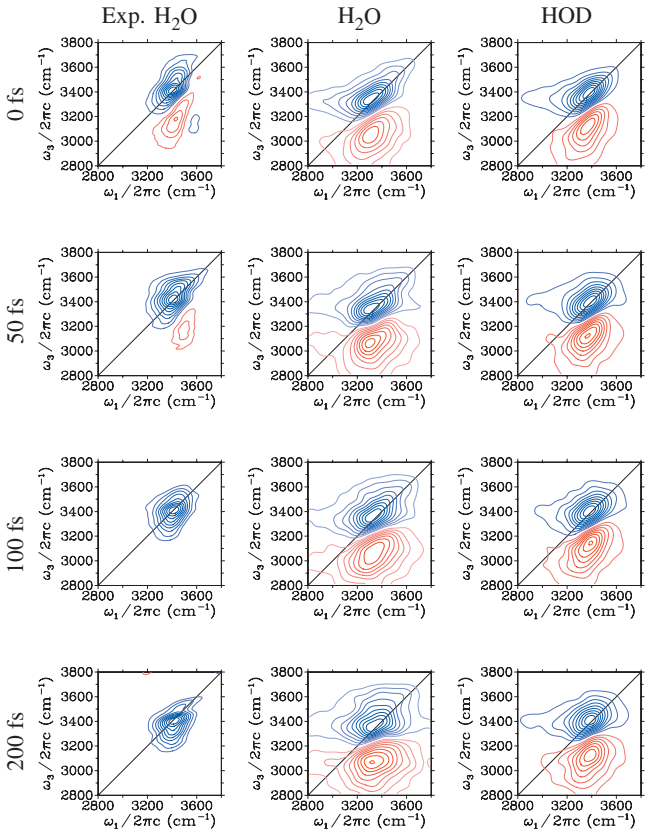


FIG. 3. The experimental 2DIR parallel-polarization spectra of bulk water from Ref. 26 (left) and the calculated 2DIR parallel-polarization spectra of bulk water (middle) and HOD in $D_2O$ (right) at different waiting times. The contours are plotted equidistantly at 10% intervals between $\pm 10\%$ and $\pm 90\%$ of the signal. Red contours indicate excited-state absorption and blue contours indicate negative absorption (bleach).

The 2DIR spectra were calculated by sampling over 100 different starting points along the trajectory. This relatively low number of realizations is sufficient since we at the same time sample over the many molecules in the simulation box, and orientation averaging for an isotropic system was also applied.[35] The spectrum was simulated for different waiting times and for both the parallel and perpendicular laser field configurations. The NISE simulations for each starting point with a fixed waiting time took about 35 h on a cluster node (Opteron 2 GHz processor). The sparse-matrix approximation was tested by varying the truncation parameter $\epsilon$. For large values of this parameter (leading to a poor approximation), a positive intensity peak showed up at $\omega_3 = 3900$ cm$^{-1}$. In the presented spectra, this artifact is completely gone. In contrast to the previous simulations,[15,16] the spectra were obtained without applying Fourier filtering to suppress noise. For comparison, an approximation to the HOD in $D_2O$ spectra, calculated by setting all couplings to zero, took 30 min (one starting point, for one waiting time) with 99% of the time-evolution matrix elements neglected. The simulated 2DIR spectra for parallel-polarized pulses are shown in Fig. 3 along with the experimental data.

In the experiment[26] the excited-state contribution disap-

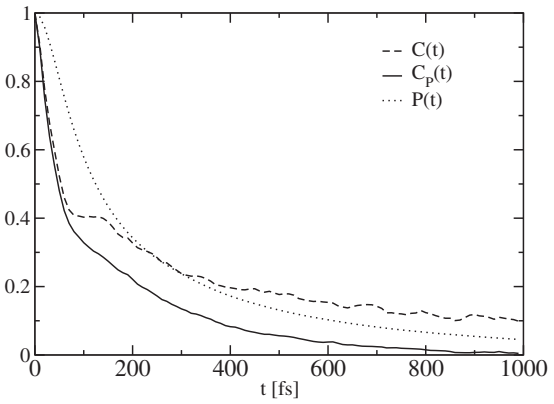


FIG. 4. The normalized frequency TCFs calculated for independent sites ($C(t)$) and including population transfer according to Eq. (12) ($C_P(t)$). The population decay, $P(t)$, is plotted as a dotted line for comparison.

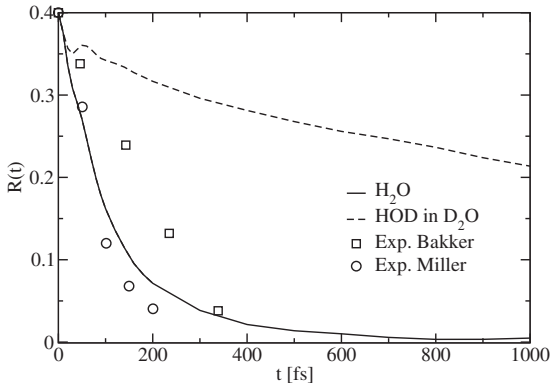


FIG. 5. The anisotropy calculated from the simulated pump-probe spectrum as in Eq. (13) (full line) compared with the result without coupling (dashed line), as would be appropriate for HOD in $D_2O$. The experimental data from Refs. 25 and 26, scaled to start at 0.4, are given with boxes and circles, respectively.

pears within 100 fs, leaving only the persistent ground-state bleach signal. This happens because the excitation can disappear into an intermediate state before returning to the ground state. For water this involves the bend vibration,[36–38] which we did not include. Therefore, the decay of the excited-state contribution and the persistent ground-state bleach is not reproduced in our simulations, which is a clear discrepancy between simulation and experiment. An *ad hoc* scheme was applied in previous simulations to catch this feature,[14] but since its precise meaning is unclear, we will not apply it here. Our spectra are very similar to those in the previous simulations,[14] although the spectral dynamics is slightly faster. At times shorter than 100 fs, the ground-state bleach/stimulated-emission peak is slightly sloped, indicating a memory of the initial excitation frequency, which disappears as a result of frequency fluctuations and population transfer. The excited-state absorption exhibits a more triangular shape, which is also observable in the experiment. The simulated spectral diffusion qualitatively agrees with the experimental data in Ref. 26. A clear tilt of the two peaks is observed at $t_2=0$ fs. The memory is lost very quickly in both cases, leaving only a small tilt at $t_2=200$ fs. Differences between theory and experiment may be due to the use of impulsive limit in the simulations, whereas the laser pulses in the experiments always have a finite duration. These pulse shape effects are most likely also the reason for the differences observed between the original[7] and the newer experiments.[26]

It is instructive to consider the differences between the theoretical spectra for $H_2O$ and for HOD in $D_2O$, as shown in Fig. 3. Recall that in the latter case the effects of intra- and intermolecular vibrational couplings are absent. One difference is that for $H_2O$ the spectra peak at slightly lower frequency, for example, at 0 waiting time, and are slightly broader, both of which reflect the effects of coherent vibrational energy transfer.[24,29] For longer waiting times, one sees slightly more peak broadening for $H_2O$, resulting from slightly more spectral diffusion. As a whole, however, the spectra in the two cases are remarkably similar. To investigate why this is so, we consider the normalized frequency TCFs, for both cases, as shown in Fig. 4. The TCF for uncoupled oscillators, from Eq. (11), as would be appropriate for HOD in $D_2O$, has lost roughly 50% of its amplitude after 50 fs, due to small-amplitude nuclear motions, and then decays on a 1 ps time scale. The TCF for the coupled oscillators, from Eq. (12), is nearly identical for the first 50 fs and then decays more quickly to zero (on the time scale of a few hundred femtoseconds), due to population transfer, which allows the excitation to sample a number of sites that may have different transition frequencies. While the behavior of these two TCFs is quite different at longer times, between 0 and 200 fs the values are not hugely different, consistent with the similar amount of spectral diffusion in the two cases, and hence the similar 2DIR spectra.

To compare with the time scale for population transfer, on the same graph we show $P(t)$ [from Eq. (9)], the probability to remain on an initial state, for the coupled system. One sees that by 200 fs a substantial amount of population transfer has occurred. It is particularly interesting that within the same time a smaller amount of population-transfer-induced spectral diffusion has occurred. We believe this is because vibrational coupling is most effective between near-resonant chromophores (those whose site frequencies differ at most by a few multiples of typical coupling matrix elements). Thus, in the frequency-domain picture,[24] eigenstates are linear combinations of near-resonant chromophores, and in the time-domain picture,[29] population transfer is most effective to near-resonant chromophores. Therefore, even though population transfer has occurred, the amount of spectral diffusion resulting from this population transfer is relatively small. Note that at longer times, about 1 ps, the cumulative effect of population transfer leads to complete spectral diffusion for the coupled system, as shown in the figure.

The tail of the population decay can be described by a biexponential decay with the time scales of 110 and 456 fs. No simple interpretation of these two time scales could be identified. The explanation might be related to the above argument that the transfer is faster when the energy difference between the oscillators is small and slower when the energy difference is large (at longer times).

In Fig. 5 we show the time-dependent anisotropy calculated with Eq. (13). It decays rapidly from an initial value of 0.4 with a $1/e$ time of 114 fs. In the experiment the initial

value is 0.35 and the decay time is $80 \pm 15$ fs.[26] In the older experiment[25] the time scale is closer to 200 fs. This can in part be due to the longer pulse duration used in those experiments. In any case, our theoretical results are in good agreement with these experiments. For comparison, in the figure we also show the anisotropy decay due to rotation alone by neglecting all couplings between chromophores (as would be appropriate for HOD in $D_2O$). It is similar to the $H_2O$ result for the first 50 fs, but then has a long tail with a time constant of 2.5 ps corresponding to the much slower rotational diffusion. For $H_2O$, only the initial drop in the anisotropy from 0.4 to 0.35 can be attributed to the orientational contribution from fast librational motion within the cone of the hydrogen-bond potential.[39] For $H_2O$, then, unlike in the situation with spectral diffusion, we see that population transfer is the dominant contributor to the anisotropy decay. Thus, even if the participating chromophores are near-resonant, producing relatively little spectral diffusion, the orientations of the transition dipoles are widely distributed, and so there is substantial anisotropy decay.

We calculated the mean-square displacement of the vibrational excitation using Eq. (10) and obtained a diffusion constant of 80 $Å^2/ps$ using the Einstein relation. This shows that from an initially excited site the excitation quickly delocalizes on neighboring sites. This diffusion constant should be compared with the diffusion constant of water molecules, which is 0.25 $Å^2/ps$ for SPC/E water[33] [the experimental value is 0.227 $Å^2/ps$ (Ref. 40)]—it is more than two orders of magnitude faster than molecular diffusion! Presumably, this in part accounts for the efficient heat dissipation in water.

## IV. CONCLUSIONS

2DIR spectra of bulk water were obtained using a new sparse-matrix algorithm within the NISE approach. The fluctuating Hamiltonian was obtained by combining MD simulations with the recently developed *ab initio* maps. The calculated spectra are in qualitative agreement with experiment, with the exception of the lack of decay of the excited-state absorption in the simulation, which is not accounted for in our approach. In addition, we calculated the rotational anisotropy decay, which is in good agreement with experiment. Keeping in mind that our approach has no adjustable parameters for the Hamiltonian and it uses the unmodified SPC/E force field, the good agreement with experiment is quite remarkable. These results provide further validation of the spectroscopic model including the intra- and intermolecular coupling maps, non-Condon effects, etc.

One of the interesting features of these experiments is that the 2DIR spectra differ by only a small amount between $H_2O$ and the uncoupled system of HOD in $D_2O$, while the anisotropy decays differ greatly. In $H_2O$ enhanced spectral diffusion and enhanced anisotropy decay are both due to population transfer as a result of the vibrational coupling. However, we argue that because only near-resonant chromophores are effectively coupled, population transfer leads to relatively little spectral diffusion during the experimentally accessible times up to 200 fs. At the same time, however, these effectively coupled near-resonant chromophores have a broad orientational distribution of transition dipoles, leading to substantial anisotropy decay.

One drawback of the presented simulations is that our approach does not account for the persistent ground-state bleach, which is rather strong in bulk water. In the future, one might want to include intermediate states such as the bend vibrations to account for this effect. Another weakness in our model is the use of simple transition dipole coupling. In particular, it is surprising that a simple transition dipole model works so well between vibrations that are separated by only a few angstroms, when the extent of the interacting electron clouds is on the order of 1 Å. Multipole effects could have a significant contribution at such short distances and models such as the extended transition dipole coupling, transition-density coupling,[41–43] or transition-charge coupling[44,45] could possibly improve the description of the intermolecular coupling. However, the intermolecular coupling used in this study was found by optimizing the transition dipole model to *ab initio* calculations, and the optimization procedure might, to some extent, compensate for the neglect of higher-order multipole contributions.

The sparse-matrix approximation to the NISE method that we introduced in this paper allows for the simulation of very big systems. With this development the calculation of 2DIR spectra for other large systems, for example, proteins and DNA, with hundreds of chromophores, is within reach. Bulk water is a strongly coupled system. The employed sparse-matrix method can be expected to work even more efficiently for more weakly coupled systems, for example, water inside reverse micelles and amide vibrations in proteins.

## ACKNOWLEDGMENTS

T.l.C.J. acknowledges the Netherlands Organization for Scientific Research (NWO) for the support through a VIDI grant. J.L.S. acknowledges support from the NSF (Grant No. CHE-0750307) and DOE (Grant No. DE-FG02-09ER16110). M.Y. acknowledges support from the Korean Research Foundation (Grant No. KRF-2008-314-C00166) and the University of Wisconsin Foundation. The authors are grateful to Dr. A. Paarmann and Dr. A. G. Dijkstra for helpful discussions. We thank Professor R. J. D. Miller and co-workers for providing their experimental data.

[1] C. W. Rella, K. D. Rector, A. Kwok, J. R. Hill, H. A. Schwettman, D. D. Dlott, and M. D. Fayer, J. Phys. Chem. **100**, 15620 (1996).
[2] P. Hamm, M. H. Lim, and R. M. Hochstrasser, J. Phys. Chem. B **102**, 6123 (1998).
[3] H. J. Bakker and J. L. Skinner, Chem. Rev. (Washington, D.C.) **110**, 1498 (2010).
[4] N. Demirdöven, C. M. Cheatum, H. S. Chung, M. Khalil, J. Knoester, and A. Tokmakoff, J. Am. Chem. Soc. **126**, 7981 (2004).
[5] H. Maekawa, C. Toniolo, A. Moretto, Q. B. Broxterman, and N.-H. Ge, J. Phys. Chem. B **110**, 5835 (2006).
[6] S. Woutersen and P. Hamm, J. Chem. Phys. **115**, 7737 (2001).
[7] M. L. Cowan, B. D. Bruner, N. Huse, J. R. Dwyer, B. Chugh, E. T. J. Nibbering, T. Elsaesser, and R. J. D. Miller, Nature (London) **434**, 199 (2005).
[8] T. L. C. Jansen and J. Knoester, Acc. Chem. Res. **42**, 1405 (2009).
[9] T. L. C. Jansen and J. Knoester, J. Phys. Chem. B **110**, 22910 (2006).
[10] R. D. Gorbunov, P. H. Nguyen, M. Kobus, and G. Stock, J. Chem. Phys.

**126**, 054509 (2007).
[11] T. L. C. Jansen and J. Knoester, Biophys. J. **94**, 1818 (2008).
[12] B. M. Auer and J. L. Skinner, J. Chem. Phys. **127**, 104105 (2007).
[13] T. la Cour Jansen and W. M. Ruszel, J. Chem. Phys. **128**, 214501 (2008).
[14] A. Paarmann, T. Hayashi, S. Mukamel, and R. J. D. Miller, J. Chem. Phys. **128**, 191103 (2008).
[15] A. Paarmann, T. Hayashi, S. Mukamel, and R. J. D. Miller, J. Chem. Phys. **130**, 204110 (2009).
[16] C. Falvo, B. Palmieri, and S. Mukamel, J. Chem. Phys. **130**, 184501 (2009).
[17] T. Hasegawa and Y. Tanimura, J. Chem. Phys. **128**, 064511 (2008).
[18] T. L. C. Jansen, J. G. Snijders, and K. Duppen, J. Chem. Phys. **113**, 307 (2000).
[19] C. P. Lawrence and J. L. Skinner, J. Chem. Phys. **117**, 5827 (2002).
[20] R. Rey, K. B. Møller, and J. T. Hynes, J. Phys. Chem. A **106**, 11993 (2002).
[21] C. J. Fecko, J. D. Eaves, J. J. Loparo, A. Tokmakoff, and P. L. Geissler, Science **301**, 1698 (2003).
[22] S. A. Corcelli, C. P. Lawrence, and J. L. Skinner, J. Chem. Phys. **120**, 8107 (2004).
[23] T. Hayashi, T. L. C. Jansen, W. Zhuang, and S. Mukamel, J. Phys. Chem. A **109**, 64 (2005).
[24] B. M. Auer and J. L. Skinner, J. Chem. Phys. **128**, 224511 (2008).
[25] S. Woutersen and H. J. Bakker, Nature (London) **402**, 507 (1999).
[26] D. Kraemer, M. L. Cowan, A. Paarmann, N. Huse, E. T. J. Nibbering, T. Elsaesser, and R. J. D. Miller, Proc. Natl. Acad. Sci. U.S.A. **105**, 437 (2008).
[27] H. Torii, J. Phys. Chem. A **110**, 9469 (2006).
[28] B. M. Auer, R. Kumar, J. R. Schmidt, and J. L. Skinner, Proc. Natl. Acad. Sci. U.S.A. **104**, 14215 (2007).
[29] M. Yang and J. L. Skinner, Phys. Chem. Chem. Phys. **12**, 982 (2010).
[30] B. M. Auer and J. L. Skinner, J. Chem. Phys. **129**, 214705 (2008).
[31] B. M. Auer and J. L. Skinner, J. Phys. Chem. B **113**, 4125 (2009).
[32] T. L. C. Jansen, D. Cringus, and M. S. Pshenichnikov, J. Phys. Chem. A **113**, 6260 (2009).
[33] H. J. C. Berendsen, J. R. Grigera, and T. P. Straatsma, J. Phys. Chem. **91**, 6269 (1987).
[34] J. E. Bertie and Z. D. Lan, Appl. Spectrosc. **50**, 1047 (1996).
[35] R. M. Hochstrasser, Chem. Phys. **266**, 273 (2001).
[36] J. C. Deàk, S. T. Rhea, L. K. Iwaki, and D. D. Dlott, J. Phys. Chem. A **104**, 4866 (2000).
[37] A. Pakoulev, Z. H. Wang, Y. S. Pang, and D. D. Dlott, Chem. Phys. Lett. **380**, 404 (2003).
[38] J. Lindner, P. Vöhringer, M. S. Pshenichnikov, D. Cringus, D. A. Wiersma, and M. Mostovoy, Chem. Phys. Lett. **421**, 329 (2006).
[39] D. E. Moilanen, E. E. Fenn, Y.-S. Lin, J. L. Skinner, B. Bagchi, and M. D. Fayer, Proc. Natl. Acad. Sci. U.S.A. **105**, 5295 (2008).
[40] K. Tanaka, J. Chem. Soc., Faraday Trans. **74**, 1879 (1978).
[41] B. P. Krueger, G. D. Scholes, and G. R. Fleming, J. Phys. Chem. B **102**, 5378 (1998).
[42] A. M. Moran, and S. Mukamel, Proc. Natl. Acad. Sci. U.S.A. **101**, 506 (2004).
[43] T. Hayashi and S. Mukamel, J. Phys. Chem. B **111**, 11032 (2007).
[44] P. Hamm and S. Woutersen, Bull. Chem. Soc. Jpn. **75**, 985 (2002).
[45] T. la Cour Jansen, A. G. Dijkstra, T. M. Watson, J. D. Hirst, and J. Knoester, J. Chem. Phys. **125**, 044312 (2006).